Stabilizing Control of a Hysteresis Cellular Neural Network Model

E.Litsyn*
Department of Mathematics, Ariel University
Atiel, Israel
elenal@gmail.com

A.Slavova *
Institute of Mathematics, Bulgarian Academy of Sciences
Sofia 1113, Bulgaria
slavova@math.bas.bg

1 Introduction

This work is devoted to mathematical modelling of pattern formation. Partial differential equations of diffusion type have long served as models for regulatory feedbacks and pattern formation in aggregates of living cells. We propose new receptor-based models for pattern formation and regulation in multicellular biological systems. The idea is that patterns are controlled by specific cell-surface receptors, which transmit to the cells signals responsible for their differentiation. The main aim of this work is to check which aspects of self-organization and regeneration can be explained within the framework of CNNs.

The simplest model describing receptor-ligand is given in the form of three equations. It takes into consideration the density of free receptors, of the bound receptors and of the ligands. We use a representation of this simplest receptor-based model that is as generic as possible and based on the scheme shown in Fig.1.

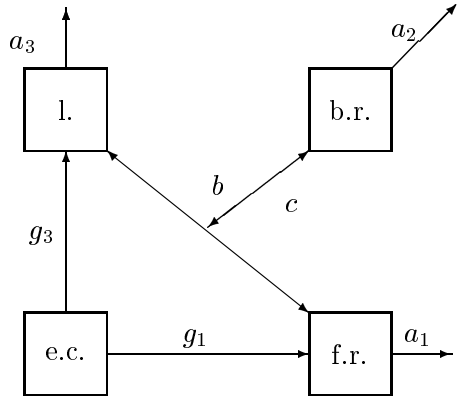

*This paper is partially supported by the bilateral joint research project between Bulgarian Academy of Sciences and Israel Academy of Sciences

Fig.1. General scheme of the simplest receptor-based model.

The abbreviations in Figure 1 are as follows: l. -ligands, b.r. - bound receptors, e.c. - epithelial cells, f.r. - free receptors. This model is based on the idea that epithelial cells secrete ligands (a regulatory biochemical), which diffuse locally within the interstitial space and bind to free receptors on the cell surface. We assume that new ligands and new free receptors are produced on cell surface through a combination of recycling (dissociation of bound receptors) and *de novo* production within the cell. Then a ligands binds to a free receptor reversibly, which results in a bound receptor that is internalised into the cell. Bound receptors also dissociate. Both ligands and free receptors undergo natural decay.

Hysteresis seems to be important in modelling biological development since according to the observation, inductive signals are present only in the certain time interval of the development. It triggers the changes in the cell's nucleus and evokes differentiation, which does not revert when signal is stopped. The developmental process is irreversible. Hysteresis results from multiple steady states. A reaction-diffusion model involving a hysteretic functional was proposed by Hopenstead and Jäger [7]. They assumed that the cell's growth had a hysteretic dependence on the amount of nutrients and acid present. Pattern formation in this model is caused by the initial instability of the ordinary differential equations (ODEs).

We consider one-dimensional epithelial sheet of length L. We denote the density of ligands by $v(x,t)$, where x and t are space and time coordinates, with x increasing from 0 to L along the body column. The density of free receptors is denoted by $u(x,t)$. Consider a system of one reaction-diffusion equation and one ordinary differential equation (ODE):

$$\left| \begin{array}{l} u_t = \Delta u + f(u,v) \\ v_t = g(u,v), \end{array} \right. \tag{1}$$

where the functions $f(u,v)$ and $g(u,v)$ present the rate of production of new free receptors and ligands, respectively and they are given by:

$$\left| \begin{array}{l} f(u,v) = -c_1 \frac{u}{1+u^2} + \frac{b_1 u}{(1+u^2-u)(1+v)} \\ g(u,v) = -c_2 \frac{v}{1+v^2} + \frac{b_2 v}{(1+v^2-v)(1+u)}, \end{array} \right. \tag{2}$$

c_1 is the rate of decay of free receptors, c_2 is the rate of decay of ligands, $b_i > 0$, $i = 1, 2$ are constants.

The systems composed of both diffusion-type and ordinary differential equations cause some difficulties, since both existence and behaviour of the solutions are more difficult to establish. Many aspects of qualitative behaviour have to be investigated numerically. For this purpose we shall apply Cellular Neural Network (CNN) approach for studying system (1),(2).

The case when $\partial_v F(u,v) \leq 0$ and $\partial_u g(u,v) \leq 0$ hold has been studied by Heinze and Schweizer [6] and they prove the existence of stationary and travelling fronts as well as they investigate the stability of these solutions.

System (1), (2) describes a receptor-based model [1] in which the production of new receptors and ligands in a steady state has a hysteretic dependence on the amount of new receptors and ligands in the sense that in a steady state the density of the new receptors and ligands is a third order polynomial divided by a second order polynomial. In [15] periodic solutions of (1), (2) has been found and existence of stationary standing wave or a spatio-temporal solution oscillating in time has been obtained numerically.

In this paper we shall study dynamical behaviour of the CNN model of (1), (2) and the emergence or complexity of the model will be proved. The edge of chaos phenomena will be presented. Then we shall design a discrete-continuous regulator of CNN model in order to stabilize the chaotic motion to an admissible solution which is connected in some way to the original behaviour of the system (1),(2).

2 Mathematical Models of Hysteresis

2.1 Hysteresis Phenomena

Hysteresis is defined in the literature as a rate independent memory effect. We shall start with an informal description of hysteresis. Consider a system whose state is characterized by two scalar variables u and v and we shall assume that they depend continuously on time t. They will play the role of independent and dependent variables, respectively. In the terminology of CNN, they are also named input and output, or also control and state, respectively.

Let us consider Fig.2 and assume the following rules. If u increases from u_1 to u_2, then the couple (u, v) moves along the curve ABC; if u decreases from u_2 to u_1, then (u, v) moves along the path CDA. Moreover, if u inverts its movement when $u_1 < u(t) < u_2$, then (u, v) moves into the interior of the region S bounded by the major loop $ABCDA$; this behaviour must be described by the specific model.

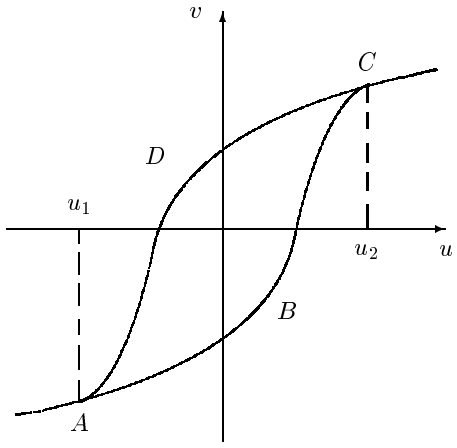

Fig.2. Hysteresis loop.

In standard examples the couple (u, v) can attain any interior point of S, by a suitable choice of the input function $u(t)$. In any case we shall assume that the

evolution of v is uniquely determined by that of u. Note that whenever $u_1 < u(t) < u_2$, $v(t)$ is not determined by the value of $u(t)$ at the same instant; indeed $v(t)$ depends on the previous evolution of u (memory effect), and possibly also on the initial state of the system.

We require that the path of the couple $(u(t), v(t))$ be invariant with respect to any increasing homeomorphism. This means that at any t, $v(t)$ depends just on the range of the restriction $u : [0, t] \to \mathbf{R}$ and on the order in which values have been attained. So there is no dependence on the derivatives of u, which may even fail to exist. Note that this condition is essential for giving a graphic representation of hysteresis in the (u, v)-plane, like in Fig. 3 : if it did not hold, the path of the couple (u, v) would depend on its velocity. In [12] this property is named **rate independence**. Therefore we shall use the following definition:

Definition 1 *Hysteresis = Rate Independence Memory Effect.*

Actually, even in most typical hysteresis phenomena, like ferromagnetism, ferroelectricity, plasticity, memory effects are not purely rate independent, since hysteresis is coupled with viscous-type effects. However, in several cases the rate independent component prevails, provided that evolution is not too fast.

Several physical phenomena exhibit hystersis. In classical continuum mechanics, hysteresis behaviour is inherent in many constitutive laws. In systems and control applications, hysteresis regularly appears via mechanical play and friction, or in the form of a relay or thermostat, often deliberately built into the system. If the hysteretic behaviour is described using a hysteresis operator, then the mathematical model for the dynamical system consists of differential equations coupled with one or several hysteresis operators, which is complemented by initial and boundary conditions. The oscillator with hystresis restoring force,

$$x''(t) + \mathcal{F}[x](t) = f(t),$$

$\mathcal{F}$ being a hysteresis operator is a basic example.

The coupling of rate independent hysteretic nonlinearities with ordinary differential equations leads to interesting mathematical problems in the theory of nonlinear oscillations. Hysteretic constitutive laws in continuum mechanics formulated in terms of hysteresis operators lead in a natural way to partial differential equations coupled with hysteresis operators, where the former represent the balance laws for mass, momentum and internal energy.

There are two types of hysteresis relations: 1).**relay** hysteresis, and 2). **active** hysteresis. In relay hysteresis, the graph (u, v) with output $v(t) = \mathcal{R}[u](t)$ moves, for a given continuous piecewise monotone input $u(t)$, on one of two fixed output curves $h_U(u)$, $h_L(u)$ defined, respectively, on $[\alpha, \infty)$, $[-\infty, \beta]$, $\alpha < \beta$ (see Fig.3), depending on which threshold, α or β, was last attained. It is known for $h_U(h_L)$ to be asymptotically constant because of saturation as $u \to +\infty(-\infty)$, and h_U, h_L need not meet. In relay hysteresis the memory-based relation can be presented by the formula:

$$\mathcal{R}[u](t) = \begin{cases} h_L(u(t)), & \text{if } u(t) \leq \alpha; \\ h_U(u(t)), & \text{if } u(t) \geq \beta; \\ h_L(u(t)), & \text{if } u(t) \in (\alpha, \beta) \quad \text{and } u(\tau(t)) = \alpha; \\ h_U(u(t)), & \text{if } u(t) \in (\alpha, \beta) \quad \text{and } u(\tau(t)) = \beta; \end{cases} \tag{3}$$

where $\tau(t) = sup\{s | s \leq t, u(s) = \alpha \text{ or } u(s) = \beta\}$. Note that $\tau(t)$ is defined for any continuous input $u(.)$, therefore the domain of $\mathcal{R}$ can be taken as $C[0, \infty)$.

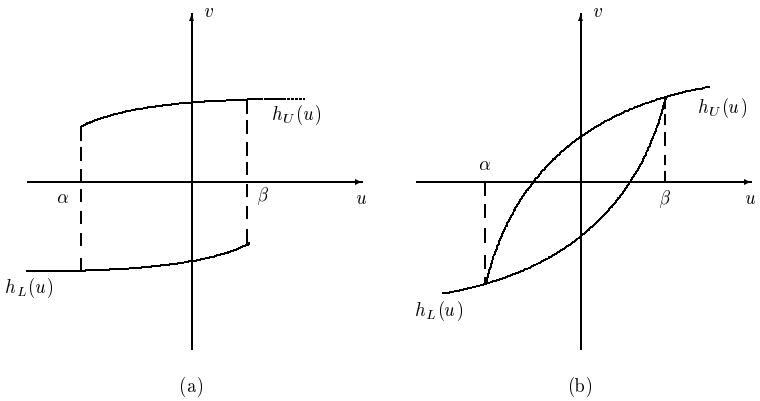

Fig. 3. Relay hystersis.

Active hysteresis allows trajectories inside the hysteresis region

$$\mathcal{H} = \{(u, v) | \alpha < u < \beta, h_L(u) < v < h_U(u)\}.$$

If the piecewise monotone input $u(t)$ increases to γ, then decreases, the graph (u, v) after $u(t) = \gamma$ moves on a response curve inside $\mathcal{H}$ (Fig.4). If the input continues to decrease to δ, then increases, the graph moves on another interior path. The mathematical models for this type of hysteresis require the existence of at least two fixed families of curves filling $\mathcal{H}$, one family for increasing $u(.)$, one family for decreasing $u(.)$. In all of the above descriptions of basic hysteresis, the relation of response to input is rate-independent, i.e. the velocity with which the input moves on the u-axis is only reflected in the velocity of the output on the v- axis. The qualitative nature of the response does not change.

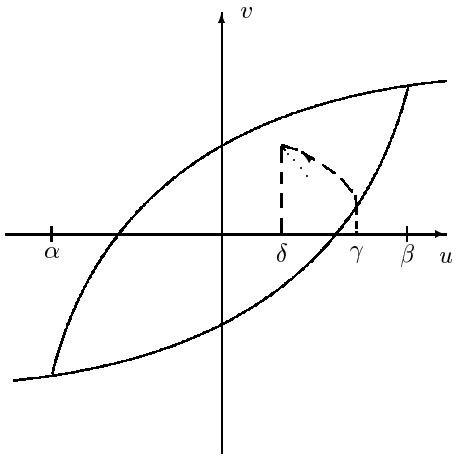

Fig. 4. Active hysteresis.

The mathematical models for the two types of hysteresis defined above are quite different, even though their memory-based behaviour is similar. Both types have been described for $u(t)$ continuous piecewise monotone, but active hysteresis is easily extended to continuous inputs by using approximations and a limit process. Relay hysteresis $\mathcal{R} : u \to \mathcal{R}[u]$ is inherently discontinuous as a map between function spaces, since an input function that just reaches a threshold and reverses just short of the threshold by an arbitrary small amount.

2.1.1 Hysteresis operators

We shall provide a functional framework for hysteresis relations and we shall introduce the concept of hysteresis operator.

Definition 2 *Hysteresis is characterized by two features:*

i). Memory - at any t, $v(t)$ may depend only on $u(t)$ but also on the previous evolution of u;

ii). Rate independence - the output is invariant with respect to changes of the time scale.

When only property i). is fulfilled, we shall speak of a memory operator.

We already indicated how the output v is constructed for a continuous and piecewise monotone input function u defined in the interval $[0, T]$. The continuity requirement is natural, whereas piecewise monotonicity is too restrictive. Here we shall show how these operators can be extended to $C^0([0, T])$. At any t, the output $v(t)$ will depend not only on $u_{[0,t]}$, but also on the initial state of the system. Hence the initial value $v(0)$, or some equivalent information; the information on $u(0)$ is clearly in $u_{[0,t]}$. So we have the following definition for the hysteresis operator $\mathcal{F}$:

$$\mathcal{F} : Dom(\mathcal{F}) \subset C^0([0, T]) \times \mathbf{R} \to C^0([0, T]). \tag{4}$$

Usually the initial state $(u(0), v(0))$ is confined to a hysteresis region $\mathcal{L}$. Then we have two possibilities: 1). the input argument $(u(0), v^0) \in \mathcal{L}$ and then $[\mathcal{F}(u, v^0)](0) = v^0$; 2). no restriction is imposed on $(u(0), v^0)$ and then the initial condition is not in the same form. In the last case, the actual initial value $[\mathcal{F}(u, v^0)](0) = v^0$ onto the interval $(\{u(0)\} \times \mathbf{R}) \cap \mathcal{L}$.

Let us now define the following properties for the hysteresis operator $\mathcal{F}$ defined above:

Causality property:

$$\begin{cases} \forall (u_1, v^0), (u_2, v^0) \in Dom(\mathcal{F}), \forall t \in]0, T], \\ \text{if } u_1 = u_2 \in [0, T], \text{ then } [\mathcal{F}(u_1, v^0)](t) = [\mathcal{F}(u_2, v^0)](t), \end{cases} \tag{5}$$

Rate independence property:

$$\begin{cases} \forall (u, v^0) \in Dom(\mathcal{F}), \forall t \in]0, T], \\ \text{if } s : [0, T] \to [0, T] \text{ is an increasing homeomorphism}, \\ \text{then } [\mathcal{F}(u \circ s, v^0)](t) = [\mathcal{F}(u, v^0)](s(t)). \end{cases} \tag{6}$$

Monotonicity properties:

Let us consider a continuous hysteresis operator (4). The standard L^2- monotonicity is defined as follows:

$$\begin{cases} \exists u_1, u_2 \in C^0([0,T]), \exists v^0 \in \mathbf{R} : \text{setting } \ v_i := \mathcal{F}(u_i, v^0), \\ \int_0^T (v_1 - v_2)(u_1 - u_2)dt < 0. \end{cases} \tag{7}$$

Next we shall define a piecewise monotonicity:

$$\begin{cases} \forall (u, v^0) \in Dom(\mathcal{F}), \forall [t_1, t_2] \subset [0,T], \\ \text{if } \ u \ \text{ is either nondecreasing or nonincreasing in } [t_1, t_2], \\ \text{then so is } \ \mathcal{F}(u, v^0); \end{cases} \tag{8}$$

that is

$$\begin{cases} \text{if } \ u, \mathcal{F}(u, v^0) \in W^{1,1}(0,T), \\ \text{then } \frac{du}{dt}\frac{d}{dt}\mathcal{F}(u, v^0) \geq 0, \end{cases} \tag{9}$$

This property is natural for rate independent operators, but there exist rate dependent operators which are continuous in $C^0([0,T])$ and fulfil (9).

2.1.2 Some mathematical models of hysteresis operators

I.Duhem hysteresis operator

The Duhem model for active hysteresis focusses on the fact that the output can only change its character when the input changes direction. This model uses an integral operator or differential equation to model the relation

$$\dot{v}(t) = f_1(v,u)\dot{u}_+(t) + f_2(v,u)\dot{u}_-(t)$$

with $\dot{u}_+(t) = max[0, \dot{u}(t)]$, $\dot{u}_-(t) = min[0, u(t)]$ to generate the curves of Fig. 5.

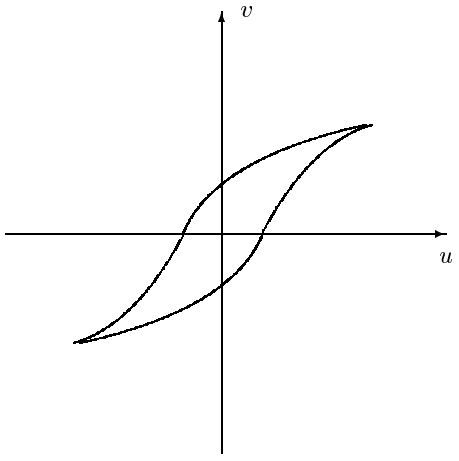

Fig.5. Duhem model.

In [12] an integral operator is considered of which a particular case is the equation

$$\frac{dv}{dt} + a|\frac{du}{dt}|g(u,v) = b\frac{du}{dt}.$$

A typical choice for g is $g(u,v) = v - b\varphi(u)$, with φ chosen so that $v(.)$ forms a classical hysteresis loop when $u(.)$ is a sinusoid.

In [12] for the Duhem model, the output is defined for piecewise monotone inputs in the following form:

$$v = \mathcal{F}[u] : \frac{dv}{dt} = \Phi(v,u,\dot{u}). \tag{10}$$

Most often, Φ is assumed to have the form

$$\Phi(v,u,\dot{u}) = \begin{cases} f_D(v,u)\dot{u}, & \dot{u}(t) \le 0; \\ f_I(v,u)\dot{u}, & \dot{u}(t) \ge 0, \end{cases}$$

with f_D, f_I continuous, D means decreasing input, I means increasing input. The solutions of (10) give the trajectories interior to the hysteresis region $\mathcal{H}$. To include C^1 boundary curves h_U and h_L, we can modify (10) by adding the constraints

$$v^{'}(t) = h_U^{'}(u(t))u^{'}(t) \text{ for } v(t) \ge h_U(u(t)),$$
$$v^{'}(t) = h_L^{'}(u(t))u^{'}(t) \text{ for } v(t) \le h_L(u(t)).$$

This adds the physically irrelevant trajectories

$$v(t) = h_L(u(t)) + c, \; v(t) = h_U(u(t)) + c$$

for initial states outside $\mathcal{H}$ and off the curves h_U, h_L.

II.Ishlinskii hysteresis operator.

It is proposed as a model for plasticity-elasticity and it is active hysteresis map whose behavior is given in Fig.6, called **stop**.

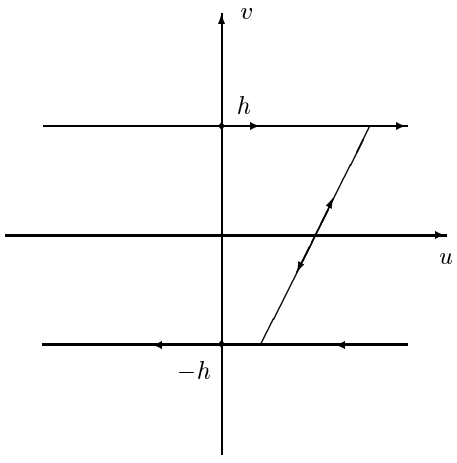

Fig.6. Ishlinskii hysteresis.

For this hysteresis the bounding curves are $v = \pm h$, the hysteresis region $\mathcal{H}$ is the strip

$$\{(u, v)| - \infty < u < \infty, -h < v < h\},$$

and the corresponding operator $S_h : u \to v$ for u continuous monotone, initial state $(u_0, v_0) \in \mathcal{H}$, according to the following rules:

i). if $u(.)$ is moving to the right at time T, then $S_h[u](t) = min\{h, u(t) - u_0 + v_0\}$;

ii). if $u(.)$ is moving left at time t, then $S_h[u](t) = max\{-h, u(t) - u_0 + v_0\}$.

The operator S_h can be defined for piecewise monotone inputs with its single interior family of two-way curves. We can describe this extension analytically by asking that the semigroup property hold:

$$S_h(t_0, v_0)[u](t) = S_h(t_1, S_h(t_0, v_0)[u](t_1))[u](t).$$

The simplest form of Ishlinskii hysteresis operator can then be defined as the superposition

$$v(t) = \mathcal{F}[u](t) \equiv \int_0^\infty \xi(h) S_h(t_0, v_0(h))[u](t) dh.$$

Although defined for piecewise monotone $u(.)$, under reasonable conditions on $\xi(.)$ ($\xi(h) \geq 0, \int^\infty h\xi(h)dh < \infty$) this operator can be extended to a map from $C(t_0, t_1)$ into $C(t_0, t_1)$; in fact Lipschitz continuous inputs will yield Lipschitz continuous outputs.

III.Preisach hysteresis model. This model uses a superposition of especially simple independent relay hysteresis operators [12]. That is,

$$\mathcal{F}[u](t) = \int\int \mu(\alpha, \beta) \hat{\mathcal{F}}_{\alpha,\beta}[u](t) d\alpha d\beta,$$

where $\mu(\alpha, \beta) \geq 0$ is a weight function, usually with support on a bounded set in the (α, β)-plane, $\hat{\mathcal{F}}_{\alpha,\beta}$ is relay hysteresis operator with thresholds $\alpha < \beta$ and

$$h_U(u) = +1 \text{ on } [\alpha, \infty);$$

$$h_L(u) = -1 \text{ on } (-\infty, \beta].$$

The arbitrary initial state $\eta = \pm 1$ must be chosen if $u(t_0) \in (\alpha, \beta)$.

The Preisach model is founded on a physical assumption: hysteresis is the result of the superposition of the behaviour of independent domains within the material , each of which can be modelled by a simple "flip-flop" relay hysteresis operator.

IV. Krasnosel'skii-Pokrovskii hysteron

Geometric approach is used to define a basic hysteresis operator, called hysteron [11]. Such hysteresis operator is first define as a "play". In this case we have $|v - u| \leq h$. This defines an active hysteresis operator with $\alpha = -\infty$, $\beta = +\infty$, and a single family of interior curves (Fig.7).

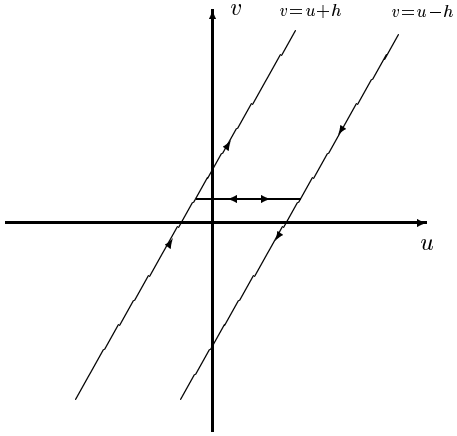

Fig.7. Krasnosel'skii-Pokrovskii hysteron.

For a given input $u(.)$, the output $v(.) \equiv P_h[u](t)$ of the play is

$$P_h[u](t) = u(t) - S_h[u](t),$$

where S_h is the stop of Fig. 6. We shall define a direct formula for P_h. Let $g_h(u,v) = min[u+h, max(u-h, v)]$. If the initial value $v_0 = v(t_0)$ is given and if the input $u(.)$ is monotone, then $P_h[u; v_0](t) = g_h(u(t), v_0)$. If $u(.)$ is piecewise monotone with $u(.)$ monotone on $I_i = [t_{i-1}, t_i]$, $i = 1, \ldots, n$, then

$$P_h[u; v_0](t) = g_h(u(t), v(t_{i-1})) \text{ for } t \in I_i.$$

Then a hysteron $\mathcal{F}$ is defined as a map from piecewise monotone continuous input function $u(.)$ to output functions $v[u](.)$. The domain $\Omega(\mathcal{F}) \subset R^2$ (the interior of which is our hysteresis region $\mathcal{H}$), which defines the input-output relation, is assumed to have the following three properties [12].

Property 1 *The intersection $K(u_0) = \Omega(\mathcal{F}) \cap l_{u_0}$ of $\Omega(\mathcal{F})$ with the vertical line $l_{u_0} = \{(u,v) | u = u_0\}$ is a nonempty interval.*

Property 2 *The endpoints of $K(u)$, $u \in R$, define two continuous curves $\Phi_L(u)$ (left endpoint) and $\Phi_R(u)$ (right endpoint). The domain of Φ_R is some interval $(-\infty, a_R)$; the domain Φ_L is some interval (b_L, ∞), $b_L < a_R$.*

Property 3 *Define $\Omega_0(\mathcal{F}) \subset \Omega(\mathcal{F})$ as the finite open region bounded by Φ_L and Φ_R; stratify this region by a given family of nonintersecting graphs of continuous functions $\pi(.)$ such that the left endpoint of each graph lies on Φ_L and the right endpoint of each graph lies on Φ_R. The remaining points of each graph do not intersect $\Phi_l \cup \Phi_R$.*

The above defines an active hysteresis operator with a single family of interior curves. They then show that any operator defined through the above properties extends uniquely from the class of piecewise monotone inputs to a mapping defined for any continuous input. Let $f(u,z)$ be a given real-valued function of two real variables continuous on $\Omega(\mathcal{F})$ and strictly monotone in z. Krasnosel'skii and Pokrovskii show that any hysteron can be represented in the form

$$\mathcal{F}[u](t) = f(u(t), P(\Gamma_L, \Gamma_R)[u](t)),$$

where $P(\gamma_L, \Gamma_R)$ is a generalized play operator defined by the hysteresis diagram in Fig. 8.

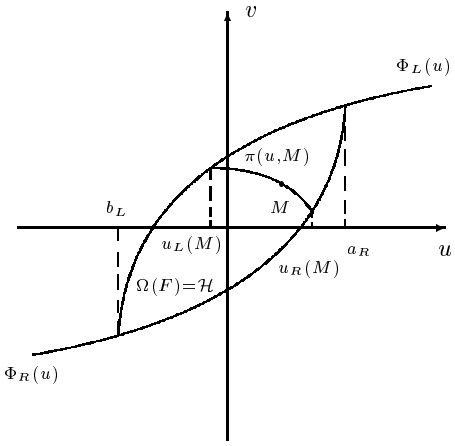

Fig.8. Play operator.

More precisely, for a generalized play we are given two continuous nondecreasing functions $\Gamma_L(u)$, $\Gamma_R(u)$ defined on respective intervals $(-\infty, a_L)$ and (b_R, ∞), $b_r < a_L$, with $\Gamma_L(u) \geq \Gamma_R(u)$ for all $b_R < u < a_L$. The two curves are connected by horizontal lines, and the output $v(.) = P(\Gamma_L, \Gamma_R)[u](.)$ for continuous monotone input $u(t)$, $t \geq t_0$, is defined as

$$v(t) = \begin{cases} max\{v(t_0, \Gamma_R[u(t)]\} & \text{when } u(t) \text{ is nondecreasing,} \\ min\{v(t_0), \Gamma_L[u(t)]\} & \text{when } u(t) \text{ is nonincreasing.} \end{cases}$$

Note that Krasnosel'skii-Pokrovskii hysteron allows a single family of interior trajectories. To allow two families Krasnosel'skii and Pokrovskii [11] define a prehysteron as any deterministic, static, weakly correct map which maps continuous piecewise monotone inputs $u(.)$ into continuous outputs $v(t) = \mathcal{F}[u](t)$. It is assumed that the initial state (u_0, v_0) at time t_0 is given and intuitively, (u_0, v_0) is in the hysteresis domain $\mathcal{H}$ or on the boundary curves.

Deterministic. $v(t) = \mathcal{F}[u](t)$, for $t \geq t_0$, is uniquely determined by $(t_0, u(t_0)$, $v(t_0)) \equiv (t_0, u_0, v_0)$ and $u(.)$.

Static. 1). $\mathcal{F}[u(.)](t)|_{(t_0,u_0,v_0)} = \mathcal{F}[u(.)](t - t_0 + t_1)|_{(t_0,u_0,v_0)}$ $(t \geq t_0)$; and

2). if we replace the input $u(t)$ by $u(\alpha t + (1-\alpha)t_0)$ with $\alpha > 0$, then the output $v(t)$ is replaced by

$$v(\alpha t + (1-\alpha)t_0) \ (t \geq t_0).$$

Weakly correct. If $\{u_n(.)\}_{n=1}^{\infty}$ and $u_*(.)$ are continuous monotone inputs, $t_0 \leq t \leq t_1$ with $(u_n(t_0), v_n^0)$ and $(u_*(t_0, v_*^0)$ admissible and if $v_n^0 \to v_*^0$, $sup_{[t_0,t_1]}|u_n(s) - u_*(s)| \to 0$, then

$$\mathcal{F}[u_n(.)](t_1)|_{(t_0,u_n(t_0),v_n)} \to \mathcal{F}[u_*(.)](t_1)|_{(t_0,u_*(t_0),v_*)}.$$

The best example of a prehysteron is a sufficiently regular Duhem model characterized by the operator in Fig 5.

3 Cellular Neural Network model

We are witnessing a technical development in our fields where the sensing, computing, activating circuits and systems are becoming inherently connected; physically and theoretically, as well. Moreover, as a result of this, our notion about sensory computing, even about computing, is in a continuous transformation. Hence, we have to make a closer look about the fundamentals of computing. How, now, can we characterize a brain-like system? We might summarize the key properties as follows:

- Continuous time continuous (analog) valued signal arrays (flows)
- Several 2Dimensional strata of analog "processors" (neurons)
- Typically, mainly local, or sparse global (bus-like) interconnections
- Sensing and processing are integrated
- Vertical interconnections between a few strata of neuron "processors"
- Variable delays
- Spatial-temporal active waves
- Events are patterns in space and/or time

These features are already strongly modifying our view and practice in building complex electronic systems, including sensing, computing, activating and communicating devices and systems. This way of thinking, however, is supposing a completely different architecture, physical and algorithmic alike, and supposes tens of thousands or millions of parallel physical processing devices.

In developing a universal and canonical computing architecture, after having been decided the forms of data, we are tending to use the simplest possible building blocks, with the simplest possible interconnections, elementary instructions and programming constructs. Then we introduce algorithmic stored programmability to make it universal and practical. A most successful example is the digital computer, with a core universal machine on integers (Turing machine). What if we would make a brain-like computer with the properties shown above? The data are topographic (image) flows. In the simplest case, a pixel array with each pixel having a light intensity of gray values between black (say, +1) and white (say, -1) values. Color pictures are composed of several pictures with different color content. A special case is a binary mask. Now, let us construct a programmable topographic cellular sensory dynamics, as implementing the protagonist elementary instruction. The recipe is as follows.

- Take the simplest dynamical system, a cell (with input u, state x and output y)
- Take the simplest spatial grid for placing the cells with the simplest neighborhood relation (2D sheets)
- Introduce the simplest spatial interactions between dynamic cells, being programmable (called cloning template or gene, or simply template)
- Add cellular sensors.

CNN is simply an analogue dynamic processor array, made of cells, which contain linear capacitors, linear resistors, linear and nonlinear controlled sources. Let us consider a two-dimensional grid with 3×3 neighborhood system as it is shown on Fig.9.

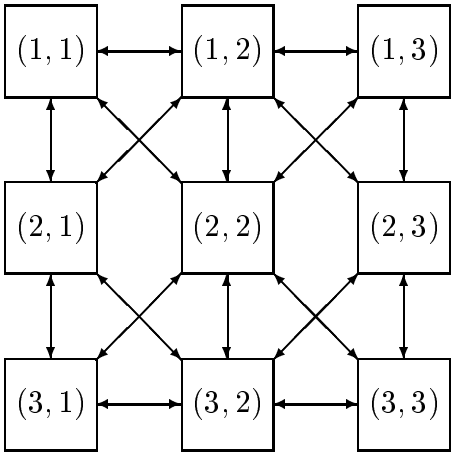

Fig.9. 3×3 neighborhood CNN.

The squares are the circuit units - cells, and the links between the cells indicate that there are interactions between linked cells.

Cellular Neural Networks (CNNs) are complex nonlinear dynamical systems, and therefore one can expect interesting phenomena like bifurcations and chaos to occur in such nets. It was shown that as the cell self-feedback coefficients are changed to a critical value, a CNN with opposite-sign template may change from stable to unstable [3]. Namely speaking, this phenomenon arises as the loss of stability and the birth of a limit cycles [3]. Moreover, the appearance of a strange attractor in a periodically driven two-cell CNN have been reported. In a three-cell autonomous CNN this attractor has properties similar to the double scroll attractor [3].

CNN [2] is simply an analogue dynamic processor array, made of cells, which contain linear capacitors, linear resistors, linear and nonlinear controlled sources. One of the key features of a CNN is that the individual cells are nonlinear dynamical systems, but that the coupling between them is linear. Roughly speaking, one could say that these arrays are nonlinear but have a linear spatial structure, which makes the use of techniques for their investigation common in engineering or physics attractive.

We will give the general definition of a CNN which follows the original one [2]:

Definition 3 *The CNN is a*

a). 2-, 3-, or n- dimensional array of

b). mainly identical dynamical systems, called cells, which satisfies two properties:

c). most interactions are local within a finite radius r, and

d). all state variables are continuous valued signals.

Definition 4 *An $M \times M$ cellular neural network is defined mathematically by four specifications:*

1). CNN cell dynamics;

2). CNN synaptic law which represents the interactions (spatial coupling) within the neighbor cells;

3). Boundary conditions;

4). Initial conditions.

Now in terms of definition 4 we can present the dynamical systems describing CNNs. For a general CNN whose cells are made of time-invariant circuit elements, each cell $C(ij)$ is characterized by its CNN cell dynamics :

$$\dot{x}_{ij} = -g(x_{ij}, u_{ij}, I^s_{ij}), \tag{11}$$

where $x_{ij} \in \mathbf{R}^m$, u_{ij} is usually a scalar. In most cases, the interactions (spatial coupling) with the neighbor cell $C(i+k, j+l)$ are specified by a CNN synaptic law:

$$\begin{aligned} I^s_{ij} &= A_{ij,kl}x_{i+k,j+l} + \tilde{A}_{ij,kl} * f_{kl}(x_{ij}, x_{i+k,j+l}) + \\ &\quad + \tilde{B}_{ij,kl} * u_{i+k,j+l}(t). \end{aligned} \tag{12}$$

The first term $A_{ij,kl}x_{i+k,j+l}$ of (12) is simply a linear feedback of the states of the neighborhood nodes. The second term provides an arbitrary nonlinear coupling, and the third term accounts for the contributions from the external inputs of each neighbor cell that is located in the N_r neighborhood.

Complete stability, i.e. convergence of each trajectory towards some stationary state, is a fundamental dynamical property in order to design CNN's for accomplishing important tasks including image processing problems, the implementation of content addressable memories and the solution of combinatorial optimization problems [5]. The most basic result on complete stability is certainly the one requiring that the CNN interconnection matrix $\tilde{A}$ be symmetric [2]. Also some special classes of nonsymmetric CNN's such as cooperative (excitory) CNN's, were shown to be completely stable [3]. In the general case, however, competitive (inhibitory) CNN's may exhibit stable nonlinear oscillations [3].

Recently, a hysteresis switch was introduced into neural networks [10,17,18]. They used hysteresis switch as cell outputs and applied them to realize an ideal associative memory. A second-order hysteresis neural network can perform both linear and nonlinear filtering in some image processing applications [14,18]. The hysteresis CNN is derived from standard CNN, and is made of first-order cells with hysteresis switches [8,9]. The hysteresis CNN cell has two operating modes-bistable multivibrator mode and relaxation oscillator mode. In the case of the bistable mode,the CNN design methodology can be applied to the hysteresis CNN. Thus, the hysteresis CNN can also perform many applications reported in the literature on CNN. In the case of the relaxation oscillator mode, the hysteresis CNN can generate various patterns and nonlinear waves. Furthermore, the hysteresis CNN has the function of both associative (static) and dynamic memories [8,9,14].

It is known [13] that some autonomous CNNs represent an excellent approximation to nonlinear partial differential equations (PDEs). In this paper we will present the receptor-based model by a reaction-diffusion CNNs. The intrinsic space distributed topology makes the CNN able to produce real-time solutions of nonlinear PDEs. Consider the following well-known PDE, generally referred to us in the literature as a reaction-diffusion equation [1]:

$$\frac{\partial u}{\partial t} = f(u) + D\nabla^2 u,$$

where $u \in \mathbf{R}^N$, $f \in \mathbf{R}^N$, D is a matrix with the diffusion coefficients, and $\nabla^2 u$ is the Laplacian operator in $\mathbf{R}^2$. There are several ways to approximate the Laplacian

operator in discrete space by a CNN synaptic law with an appropriate A-template [13,14].

Now, let us map the functions $u(x,t)$ and $v(x,t)$ from (1), (2) into a 2-dimensional grids. Then we approximate each function by a set of functions $u_j(t)$ and $v_j(t)$ which are defined as

$$u_j(t) = u(jh_x, t),$$
$$v_j(t) = v(jh_x, t),$$

where h_x is the space interval in x. Then the Laplacian Δu in (1) will be approximated by $\Delta u \approx u_{j-1}(t) - 2u_j(t) + u_{j-1}(t)$. So, in our particular case for the model with hysteresis (1), (2) we shall take one-dimensional discretized Laplacian template:

$$A : (1, -2, 1)$$

Therefore the CNN representation for our hysteresis model (1), (2) will be the following:

$$\begin{aligned} \frac{du_j}{dt} &= (u_{j-1} - 2u_j + u_{j+1}) + \\ &+ f(u_j, v_j) \\ \frac{dv_j}{dt} &= g(u_j, v_j), 1 \le j \le N. \end{aligned} \tag{13}$$

The above system is actually a system of ODE which is identified as the state equation of an autonomous CNN made of N cells. For the output of our CNN model (13) we will take the standard sigmoid function [2].

4 Edge of chaos in the hysteresis CNN model

The theory of local activity provides a definitive answer to the fundamental question: what are the values of the cell parameter for which the interconnected system may exhibit complexity? The answer is given in [4] - the necessary condition for a nonconservative system to exhibit complexity is to have its cell locally active. The theory which will be presented below and which follows [4] offers a constructive analytical method for uncovering local activity. In particular, for diffusion CNN model, one can determine the domain of the cell parameters in order for the cells to be locally active, and thus potentially capable of exhibiting complexity. This precisely defined parameter domain is called the edge of chaos [4].

We apply the following constructive algorithm:

1. Map hysteresis model (1), (2) into the following associated discrete-space version which we shall call hysteresis CNN model:

$$\begin{aligned} \frac{du_j}{dt} &= (u_{j-1} - 2u_j + u_{j+1}) + \\ &+ f(u_j, v_j) = U + f \\ \frac{dv_j}{dt} &= g(u_j, v_j) = g, 1 \le j \le N. \end{aligned} \tag{14}$$

2. Find the equilibrium points of (14). According to the theory of dynamical systems, the equilibrium points (u^e, v^e) of (14) are these for which:

$$\begin{aligned} U + f(u^e, v^e) &= 0, \\ g(u^e, v^e) &= 0. \end{aligned} \tag{15}$$

If we substitute (2) into (15), we obtain:

$$\begin{aligned} U - c_1 \frac{u^e}{1 + (u^e)^2} + \frac{b_1 u^e}{(1 + (u^e)^2 - u^e)(1 + v^e)} &= 0 \\ -c_2 \frac{v}{1 + (v^e)^2} + \frac{b_2 v^e}{(1 + (v^e)^2 - v^e)(1 + u^e)} &= 0.. \end{aligned} \tag{16}$$

After solving (16), we obtain that it has one, two or three real roots $E_1 = (u_1^e, v_1^e)$, $E_2 = (u_2^e, v_2^e)$, $E_3 = (u_3^e, v_3^e)$, respectively. In general, these roots are finctions of the cell parameters $c_{1,2}$ and $b_{1,2}$.

3. We calculate now the four cell coefficients of the Jacobian matrix of (16) about each system equilibrium point E_i, $i = 1, 2, 3$:

$$\left[\begin{array}{cc} \frac{\partial f(u,v)}{\partial u} & \frac{\partial f(u,v)}{\partial v} \\ \frac{\partial g(u,v)}{\partial u} & \frac{\partial g(u,v)}{\partial v} \end{array} \right] |_{(u,v)=E_i, i=1,2,3} = \left[\begin{array}{cc} f_1^e & f_2^e \\ g_1^e & g_2^e \end{array} \right]. \tag{17}$$

4. Calculate the trace $Tr(E_i)$ and the determinant $\Delta(E_i)$ of the Jacobian matrix (17) for each equilibrium point:

$$\begin{aligned} Tr(E_i) &= f_1^e(E_i) + g_2^e(E_i), \\ \Delta(E_i) &= f_1^e(E_i) g_2^e(E_i) - f_2^e(E_i) g_1^e(E_i). \end{aligned} \tag{18}$$

5. We shall identify the cell state variables u_j and v_j as follows: u_j is associated with the node-to-datum voltage at node j of a grid G_1 of linear resistors; v_j is associated with the node-to-datum voltage at node j of a second grid G_2. We identify the coupling input U with the current leaving node j, i.e. entering the cell connected to node j. In this case, the associated electronic circuit has three terminals with two node-to-datum voltages (u_j, v_j) and one terminal current U [3,4]. The importance of the circuit model is not only in the fact that we have a convenient physical implementation, but also in the fact that well-known results from classic circuit theory can be used to justify the cells' local activity [4]. In this sense, if there is at least one equilibrium point for which the circuit model of the cell acts like a source of "small signal", in a precise sense defined in [4], i.e. if the cell is capable of injecting a net small-signal average power into the passive resistive grids, then the cell is said to be locally active.

Definition 5 *A diffusion cell is locally active at an equilibrium point E_i, iff the matrix:*

$$L_{E_i} = \left[\begin{array}{cc} -2f_1^e & -(f_2^e + g_1^e) \\ -(f_2^e + g_1^e) & -2g_2^e \end{array} \right] \tag{19}$$

is not positive semi-definite at the equilibrium point E_i, $i = 1, 2, 3$.

Remark 1 A matrix M is called positive semi-definite if $x^*MX \geq 0$ for all $x \in \mathbf{R}^n$, where x^* denotes the conjugate transpose of x.

Definition 6 *Local activity region $LAR(E_i)$ is defined as follows:*

$$LAR(E_i) : g_2^e > 0 \quad 4f_1^e g_2^e < (f_2^e + g_1^e)^2, i = 1, 2, 3. \tag{20}$$

Definition 7 *Stable and locally active region $SLAR(E_i)$ at the equilibrium point E_i for the hysteresis CNN model (14) is such that $Tr < 0$ and $\Delta > 0$.*

6. Edge of chaos

In the literature [3,4], the so-called edge of chaos (EC) means a region in the parameter space of a dynamical system where complex phenomena and information processing can emerge. We shall try to define more precisely this phenomena till now known only via empirical examples. Moreover, we shall present an algorithm for determining the edge of chaos for diffusion CNN models as our hysteresis CNN model (14). Let us set $U = 0$ in the equilibrium equations:

$$\begin{aligned} U + f(u^e, v^e) &= 0, \\ g(u^e, v^e) &= 0. \end{aligned} \tag{21}$$

After solving the above system we get that it can have one, two or three real solutions and therefore we have three equilibrium points $E_i(u_i^e, v_i^e)$, $i = 1, 2, 3$.

Our next step is to calculate the local cell coefficients f_1^e, f_2^e, g_1^e, g_2^e from (16) about each equilibrium point E_i, $i = 1, 2, 3$. We determine LAR and SLAR for each point in the cell parameter space and we found that there is at least one equilibrium point $E(0, 0)$ for which these conditions hold. We shall identify the edge of chaos domain EC in the cell parameter space by using the following definition [4]:

Definition 8 *A hysteresis CNN is said to be operating on the edge of chaos EC iff there is at least one equilibrium point E_i, $i = 1, 2, 3$ which is both locally active and stable when $U = 0$.*

The following theorem then hold:

Theorem 1 *Hysteresis CNN model for the system (1), (2) is operating in the edge of chaos regime iff $c_1 > b_1 > 0$, $c_2 > b_2 > 0$. For this parameter values, there is at least one equilibrium point which is both locally active and stable.*

Proof: After solving (21) we have three equilibrium points $E_1 = (0, 0)$, $E_2 = (-1, -1)$ and $E_3 = (-1, \frac{-2b_1 - 3c_1}{3c_1})$. Then we check the conditions for local activity and stability given by Definitions 4,5. The results show that the equilibrium point $E_1 = (0, 0)$ satisfy these conditions for the following parameter set $c_1 > b_1 > 0$ and $c_2 > b_2 > 0$. Therefore, there is at least one equilibrium point which is both locally active and stable. According to Definition 6, this means that the hysteresis CNN model (14) is operating in the edge of chaos regime [4]. Theorem is proved.

Here in this paper we shall perform simulations for the receptor-based CNN model (7). We obtain the following figures:

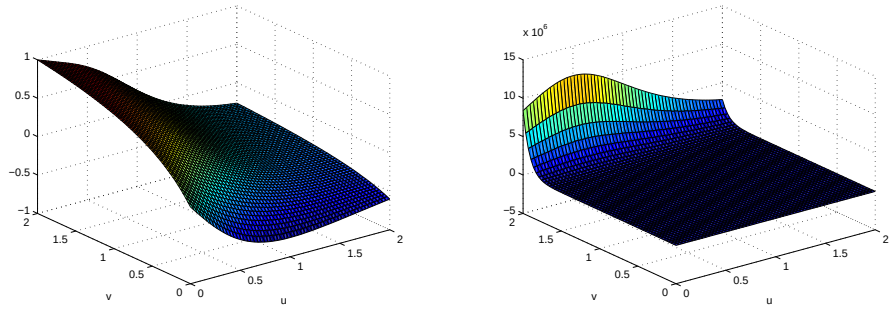

Fig.10. Stationary wave solution of the receptor-based CNN model for the following parameter set:$c_i, b_i \in [1,2], i = 1,2$.

We can see from Fig. 10 that for small enough diffusion coefficients what is equal to the large enough domain size, we have formation of inhomogeneous solutions (fronts) which are stationary in time.

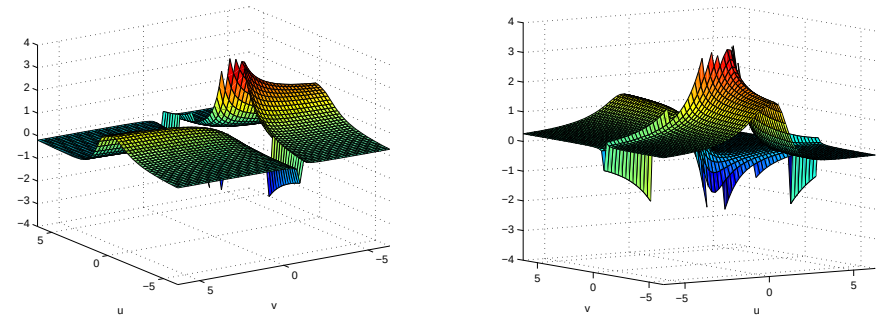

Fig.11. Spatio-temporal solution of the receptor-based CNN model for the following parameter set: $c_i, b_i \in [1,2], i = 1,2$.

Simulations show that for the model (14) we can have a gradient-like solution for the density of free receptors (standing wave) which is stationary in time (see Fig.10) or a spatio-temporal solution oscillating in time (see Fig. 11). The hysteresis CNN cell [11] has two operating modes, namely, a bistable multivibrator mode and a relaxation oscillator mode. In the case of the bistable mode, the CNN gene design methodology [3] can be applied to hysteresis CNN. In the case of relaxation oscillator mode, the hysteresis CNN can generate various patterns and nonlinear waves. Furthermore, the hysteresis CNN has the function of both associative (static) and dynamic memories. The formation and persistence of the several peaks on Fig.11 are result of the bistability of the reaction term. For such model we can have various stable solutions which are transitions between the stable steady states.

Remark 2 There are essentially two ways in which a system of identical cells can start to differentiate:

1). There is a critical number of cells (size of domain), above which the spatially homogeneous attractors loses stability, which leads to "spontaneous" spatial pattering. It is the case of Turing-type instability [16]. Such models can explain the *de*

novo pattern formation since for some set of parameters domain size value, the final pattern is the same and does not depend on the initial perturbation.

2). There is an external inducing signal which drives the system into new, spatially inhomogeneous state. Such signal originates from another group of already differentiated cells. In such case the signal must be strong enough to trigger differentiation. It corresponds to a sufficiently strong initial perturbation of the homogeneous steady state. This type of the initialization of the pattern-forming mechanism is involved in the models with hysteresis.

5 Continuous feedback control of the CNN model

Let us rewrite the CNN model (14) by the following simultaneous $2 * N$ ordinary differential equations:

$$\begin{aligned} \frac{du_j}{dt} &= (u_{j-1} - 2u_j + u_{j+1}) + \\ &+ f(u_j, v_j) + z_{uj}, j = 1 \dots N, \\ \frac{dv_j}{dt} &= g(u_j) + z_{vj}, j = 1 \dots N, \end{aligned} \tag{22}$$

where z_{uj}, z_{vj} are controls and

$$\left| \begin{array}{l} f(u,v) = -c_1 \frac{u}{1+u^2} + \frac{b_1 u}{(1+u^2-u)(1+v)} \\ g(u,v) = -c_2 \frac{v}{1+v^2} + \frac{b_2 v}{(1+v^2-v)(1+u)}, \end{array} \right. \tag{23}$$

Numbers of cells N lies in bounds $1 \leq N \leq 25$. Constant coefficients

$$c_j \in [0,1], b_j \in [1,2]. \tag{24}$$

Boundary conditions for (22) are

$$u(t,-1) = u(t,N+1) = 0$$

and initial conditions are in the intervals

$$u(0,j) \in [0,2], v(0,j) \in [0,2].$$

The matrix form of (22) is

$$\begin{aligned} \frac{dU}{dt} &= AU + F(U,V) + Z_U, \\ \frac{dV}{dt} &= G(U,V) + Z_V \end{aligned} \tag{25}$$

where the triagonal $N \times N$ matrix

$$A = \begin{bmatrix} -2 & 1 & 0 & \dots & \dots & \dots & 0 \\ 1 & -2 & 1 & 0 & \dots & \dots & 0 \\ \dots & \dots & \dots & \dots & \dots & \dots & \dots \\ 0 & \dots & \dots & 0 & 1 & -2 & 1 \\ 0 & \dots & \dots & \dots & 0 & 1 & -2 \end{bmatrix}. \tag{26}$$

The nonlinear state model of (22) is in the following matrix form

$$\frac{dX}{dt} = A_e X + F_e(X) + Z \tag{27}$$

in which the block matrices are

$$X = \begin{bmatrix} U \\ V \end{bmatrix}, F_e = \begin{bmatrix} F \\ G \end{bmatrix}, Z = \begin{bmatrix} Z_U \\ Z_V \end{bmatrix}, A_e = \begin{bmatrix} A & 0_{N\times N} \\ 0_{N\times N} & 0_{N\times N} \end{bmatrix}. \tag{28}$$

Linearized model of (27) in the neighborhood of the equilibrium point X_s is

$$\frac{dX}{dt} = (A_e + F_{Xe}(X_s))X + Z, \tag{29}$$

where

$$F_{Xe}(X_s) = \frac{\partial F_e(X_s)}{dX} = \begin{bmatrix} \frac{\partial F(X_s)}{\partial U} & \frac{\partial F(X_s)}{\partial V} \\ \frac{\partial G(X_s)}{\partial U} & \frac{\partial G(X_s)}{\partial V} \end{bmatrix}. \tag{30}$$

At the equilibrium point $E_1 = (0, 0)$ the coefficient matrix of linearized system (29) takes the form

$$A_e + F_{Xe}(X_s) = \begin{bmatrix} A + (b_1 - c_1)E & 0_{N\times N} \\ 0_{N\times N} & (b_2 - c_2)E \end{bmatrix}. \tag{31}$$

It follows from (31) that the eigenvalues $\{\lambda_j^0, j = 1 \dots 2N\}$ of the linearized system (29) are

$$\begin{aligned} \lambda_j^0 &= \lambda_j + b_1 - c_1, \quad j = 1 \dots N; \\ \lambda_{N+1}^0 &= \dots = \lambda_{2N}^0 = \mu^0 = b_2 - c_2, \end{aligned} \tag{32}$$

where λ_j, $j = 1 \dots N$ are the eigenvalues of the matrix A (18).

We shall seek stabilized controls for (29), (31) as follows

$$Z_U = k_u V, \quad Z_V = k_v U + k_w V, \tag{33}$$

where the values of the scalar control coefficients k_u, k_v, k_w are to be found. The close-loop system (29), (31), (33) have the matrix representation

$$\frac{dX}{dt} = (A_e + F_{Xe}(X_s) + R)X, \tag{34}$$

where

$$R = \begin{bmatrix} 0_{N\times N} & k_u E \\ k_v E & k_w E \end{bmatrix}.$$

So we obtain the following close-loop system's dynamical matrix

$$A_{cl} = \begin{bmatrix} A + (b_1 - c_1)E & k_u E \\ k_v E & (k_w - b_2 - c_2)E \end{bmatrix} \tag{35}$$

Characteristic polynomial of (35) is

$$det(sE - A_{cl}) = det \begin{bmatrix} (s - b_1 + c_1)E - A & -k_u E \\ -k_v E & (s - k_w - b_2 + c_2)E \end{bmatrix}$$

$$= det(\begin{bmatrix} (s - b_1 + c_1)E - A & -k_u E \\ -k_v E & (s - k_w - b_2 + c_2)E \end{bmatrix} \times$$

$$\times \begin{bmatrix} E & 0_{N\times N} \\ \frac{k_v}{s - k_w - b_2 + c_2} E & E \end{bmatrix})$$

$$= det \begin{bmatrix} (s - b_1 + c_1 - \frac{k_u k_v}{s - b_2 + c_2})E - A & -k_u E \\ 0_{N\times N} & (s - k_w - b_2 + c_2)E \end{bmatrix}$$

$$= (s - k_w - b_2 + c_2)^N \cdot det[(s - b_1 + c_1 - \frac{k_u k_v}{s - k_w - b_2 + c_2})E - A]$$

$$= (s - k_w - b_2 + c_2)^N \cdot det[\frac{(s - b_1 + c_1)(s - k_w - b_2 + c_2) - k_u k_v}{s - k_w - b_2 + c_2})E - A].$$

Let matrix A has m eigenvalues λ_j of order m_j, $j = 1 \dots m$. So the characteristic polynomial of A is

$$det[sE - A] = \prod_{j=1}^{m} (s - \lambda_j)^{m_j}.$$

Then the characteristic polynomial of (35) can be represented as

$$det(sE - A_{cl}) = \prod_{j=1}^{m} [(s - b_1 + c_1 - \lambda_j)(s - k_w - b_2 + c_2) - k_u k_v]^{m_j} \tag{36}$$

As it follows from (32), (36) the eigenvalues $\{\lambda_j^{cl}, j = 1 \dots 2N\}$ of the close-loop system (29),(31),(33) are solutions of the equations

$$(s - \lambda_j^0)(s - k_w - \mu^0) - k_u k_v = 0, j = 1 \dots N,$$

or, after some trivial algebraic calculations,

$$s^2 - (k_w + \mu^0 + \lambda_j^0)s + [\lambda_j^0(k_w + \mu^0) - k_u k_v] = 0, j = 1 \dots N. \tag{37}$$

The next theorem gives the opportunity to find feedback coefficients (32) for the stabilizing close-loop system (34) and in addition ensures the designed rate of convergence.

Theorem 2 *If the parameters of the close-loop system (34) with open-loop eigenvalues (32) satisfy the following inequalities*

$$\begin{aligned} k_w &\leq -2\sigma - \mu^0 - max_j(\lambda_j^0) \\ k_u k_v &\leq \sigma^2 + \sigma(k_w + \mu^0) + min_j \lambda_j^0(\sigma + k_w + \mu^0) \end{aligned} \tag{38}$$

for some $\sigma \geq 0$, then eigenvalues of the close-loop system satisfy the inequality $\lambda_j^{cl} \leq -\sigma$. For each value of $\sigma \geq 0$ exist values of control feedback parameters (33), for which the inequalities (38) are satisfied.

Proof: It is well known, that positivity of coefficients is the necessary and sufficient condition for a second - order polynomial to be Hurwitz. Let us shift a polynomial argument s by $\sigma > 0$ to the left. It is obvious, that the Hurwitz property of the shifted polynomial implies that the roots $s_i$of the initial polynomial satisfy inequality $s_i < \sigma$. Let us perform in the characteristic equations (37) of the close-loop system change of variable s to $s - \sigma$:

$$s^2 - (2\sigma + k_w + \mu^0 + \lambda_j^0)s + [\sigma^2 + \sigma(k_w + \mu^0 + \lambda_j^0) + \lambda_j^0(k_w + \mu^0) - k_u k_v] = 0.$$

Then the conditions $\lambda^{cl} \leq -\sigma$ are satisfied if and only if the following inequalities

$$k_w \leq -2\sigma - \mu^0 - \lambda_j^0, k_u k_v \leq \sigma^2 + \sigma(k_w + \mu^0) + \lambda_j^0) + \lambda_j^0(k_w + \mu^0)$$

hold for every eigenvalue λ_j^0, $j = 1 \ldots N(32)$ of the open-loop system. Replacing the right-hand parts of these inequalities by there least value according to j, we obtain (38). The rest of the proof follows immediately from the form of the inequalities.

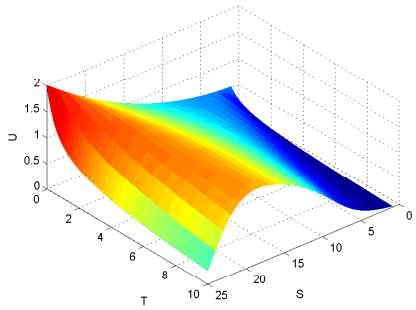

Fig.12. Spatio-temporal solution of the unstabilized receptor-based CNN model.

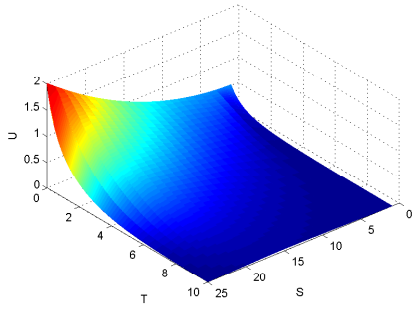

Fig.13. Spatio-temporal solution of the stabilized receptor-based CNN model, $\sigma = 0.5$.

As in can be seen from figures 12 and 13, the proposed method allows so to stabilize the system's dynamics so to assign its rate of convergence.

6 Conclusions

This paper is devoted to mathematical modelling of pattern formation. In particular, the system describing our receptor-based model (Fig.1) is composed of both diffusion-type and ordinary differential equations. Such systems are quite difficult to be studied qualitatively and for this reason we propose CNN approximation of the model. Many aspects of qualitative behaviour have to be investigated numerically. We found new patterns of behaviour of the solutions of our system (1), (2) (see Fig.11). As in many other cases the complexity of the biological process makes it difficult to give a rigorous derivation of the solutions. For this reason we propose the algorithm based on the local activity theory in order to study dynamical behaviour of the system (1), (2).

We consider in this paper the mechanism of pattern formation which results from the existence of multiple steady states due the hysteresis type nonlinearity. In the simulations of our CNN model we show that stationary fronts can arise in such models, however, the dynamics of the complete system is more complicated and we observe also spatio-temporal patterns (oscillating in time) Fig.11. In this way we have shown that in the systems with hysteresis many inhomogeneous steady states can coexist. By introducing memory to the model we allow the system to jump from one stable steady state to another when the density of receptors and ligands is varied. Assuming small values of the diffusion coefficients we obtained spatial heterogenity in the densities of substances considered.

References

[1] N.F.Britton, *Reaction-Diffusion Equations and Their Applications to Biology*, New York: Academic, 1986.

[2] L.O.Chua, L.Yang, "Cellular Neural Network: Theory and Applications", *IEEE Trans. CAS*, vol. 35, pp. 1257-1290, Oct. 1988.

[3] L.O. Chua, CNN:A Paradigm for Complexity, World Scientific Series on Nonlinear Science, Series A, vol. 31, World Scientific, Singapore, 1988.

[4] L.O.Chua,Local activity in the origin of complexity, Int.J.Biffurcations and Chaos, 2005.

[5] L.O.Chua, M.Hasler, G.S.Moschytz, J.Neirynsk, "Autonomous cellular neural networks: a unified paradigm for pattern formation and active wave propagation", *IEEE Trans. CAS-I*, vol. 42, N 10, pp. 559-577, Oct. 1995.

[6] S.Heinze, B.Schweizer, "Creeping fronts in degenerate reaction-diffusion systems", to appear.

[7] F.Hoppensteadt, W.Jäger, "Pattern formation by bacteria". In S.Levin, editor, *Lecture Notes in Biomathematics:Biological Growth and Spread*, pp. 69-81, Heidelberg, Springer-Verlag,1980.

[8] M.Itoh, L.O.Chua, "Designing CNN genes", *Int.J.Bifurcation and Chaos*, 13, 2739-2824, 2003.

[9] M.Itoh, L.O.Chua, "Star cellular neural networks for associative and dynamical memories", *Int.J.Bifurcation and Chaos* 14, 1725-1772, 2004.

[10] K.Jinno, T.Saito, "Analysis and synthesis of continuous time hysteric neural networks", *Trans. IEICE* J75-A, 552-556, 1992.

[11] M.A.Krasnosel'skii, A.V.Pokrovskii,*Systems with Hysteresis*, Nauka, Moskow, 1983. 1989; English translation of Sistemy s Gisterezisom, Springer-Verlag, Berlin, New York.

[12] Macki J., Nistri P., Zecca P., Mathematical models for hysteresis, SIAM Review, 1993; 53:1:94-123.

[13] T.Roska, L.O.Chua, D.Wolf, T.Kozek, R.Tetzlaff, F.Puffer, "Simulating nonlinear waves and partial differential equations via CNN- Part I: Basic techniques", *IEEE Trans. CAS-I*, vol. 42, N 10, pp. 807-815, Oct. 1995.

[14] A.Slavova, *Cellular Neural Networks: Dynamics and Modeling*, Kluwer Academic Publishers, 2003.

[15] A.Slavova, M.Markova, Receptor-based CNN Model with Hysteresis for Pattern Formation, Proc. IEEE, CNNA 2006, pp. 241-244, 2006.

[16] A.M.Turing, "The chemical basis of morphogenesis", *Phil.Trans.Roy.Soc. B*, 237:37-72, 1952.

[17] L. Wang, J.Ross, "Synchronous neural networks of nonlinear threshold elements with hysteresis," Proc. National Academy of Sciences (USA), vol. 87, pp. 988 - 992, 1990.

[18] L.Wang, "Suppressing chaos with hysteresis in a higher order neural network," IEEE Transactions on Circuit and Systems-II: Analog and Digital Signal Processing, vol. 43, no. 12, pp. 845-846, December, 1996.